AD-A152 334 THE SOLAR CORONAL X-RAY SPECTRUM 55-12 A(U) AEROSPACE CORP EL SEGUNDO CA SPACE SCIENCES LAB D L MCKENZIE ET AL. 01 MAR 85 TR-0084A(5940-01)-1 1/1

UNCLASSIFIED SD-TR-85-07 F04701-83-C-0084 F/G 3/2 NL

END

DATE FILMED

5 85

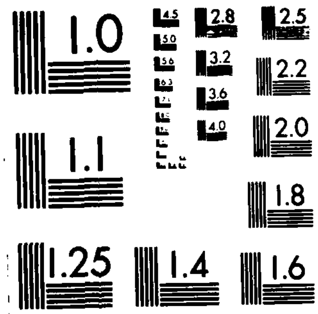

MICROCOPY RESOLUTION TEST CHART
NATIONAL BUREAU OF STANDARDS-1963-A

AD-A152 334

REPORT SD-TR-[illegible]

The [illegible]

[illegible]

85 03 22 001

This report was submitted by The Aerospace Corporation, El Segundo, CA 90245, under Contract No. F04701-83-C-0084 with the Space Division, P.O. Box 92960, Worldway Postal Center, Los Angeles, CA 90009-2960. It was reviewed and approved for The Aerospace Corporation by H. R. Rugge, Director, Space Sciences Laboratory. First Lieutenant Douglas R. Case, SD/YCC, was the Project Officer for the Mission Oriented Investigation and Experimentation Program.

This report has been reviewed by the Public Affairs Office (PAS) and is releasable to the National Technical Information Service (NTIS). At NTIS, it will be available to the general public, including foreign nationals.

This technical report has been reviewed and is approved for publication. Publication of this report does not constitute Air Force approval of the report's findings or conclusions. It is published only for the exchange and stimulation of ideas.

Douglas R. Case

Douglas R. Case, 1st Lt, USAF
Project Officer

Joseph Hess

Joseph Hess, GM-15, Director, West Coast
Office, AF Space Technology Center

UNCLASSIFIED

SECURITY CLASSIFICATION OF THIS PAGE (When Data Entered)

REPORT DOCUMENTATION PAGE

READ INSTRUCTIONS BEFORE COMPLETING FORM

1. REPORT NUMBER SD-TR-85-07	2. GOVT ACCESSION NO. AD-A152	3. RECIPIENT'S CATALOG NUMBER 334
4. TITLE (and Subtitle) THE SOLAR CORONAL X-RAY SPECTRUM 5.5-12 Å		5. TYPE OF REPORT & PERIOD COVERED
		6. PERFORMING ORG. REPORT NUMBER TR-0084A(5940-01)-1
7. AUTHOR(s) D. L. McKenzie, P. B. Landecker, U. Feldman, and G. A. Doschek		8. CONTRACT OR GRANT NUMBER(s) F04701-83-C-0084
9. PERFORMING ORGANIZATION NAME AND ADDRESS The Aerospace Corporation El Segundo, Calif. 90245		10. PROGRAM ELEMENT, PROJECT, TASK AREA & WORK UNIT NUMBERS
11. CONTROLLING OFFICE NAME AND ADDRESS Space Division Los Angeles Air Force Station Los Angeles, Calif. 90009-2960		12. REPORT DATE 1 March 1985
		13. NUMBER OF PAGES 38
14. MONITORING AGENCY NAME & ADDRESS (if different from Controlling Office)		15. SECURITY CLASS. (of this report) Unclassified
		15a. DECLASSIFICATION/DOWNGRADING SCHEDULE

16. DISTRIBUTION STATEMENT (of this Report)

Approved for public release; distribution unlimited.

17. DISTRIBUTION STATEMENT (of the abstract entered in Block 20, if different from Report)

18. SUPPLEMENTARY NOTES

19. KEY WORDS (Continue on reverse side if necessary and identify by block number)

Sun: corona,
Sun: flares,
Sun: spectra,
Sun: X rays.

20. ABSTRACT (Continue on reverse side if necessary and identify by block number)

Solar X-ray spectra in the wavelength range 5.5-12 Å have been measured by the SOLEX spectrometers aboard the USAF P78-1 satellite. The spectra were measured under a variety of flaring and nonflaring conditions. High sensitivity, attained by summing data from several successive spectral scans, enabled the detection of 85 lines, 22 of which remain unidentified, in this wavelength range. In addition, observations of many strong lines were possible with individual scans during the course of the flare evolution. This capability, coupled with the availability of nonflare spectra,

cont

DD FORM 1473 (FACSIMILE)

UNCLASSIFIED

SECURITY CLASSIFICATION OF THIS PAGE (When Data Entered)

19. KEY WORDS (Continued)

20. ABSTRACT (Continued)

facilitated the identification of several lines. The lines of Fe XXII-XXIV are especially important in this wavelength range. For many of these lines, theoretical and observed line strengths were compared. In some cases the agreement was good and in others it was not. For each of these ions, n = 4-2 transitions were detected. While relatively weak, these lines have the advantage of being unblended. They may be diagnostically useful in the future when theoretical calculations are available. Diagnostically valuable line ratios were evaluated for the helium-like species Mg XI, Al, XII, and Si XIII. The density-sensitive ratio, R, was found to agree with theoretical calculations of the low density limiting value for both Mg XI and Si XIII, the only species for which it was measured. In all cases, the ratio G was lower than calculated values.

cont keywords include: [illegible]

CONTENTS

Accession For
NTIS GRA&I
DTIC TAB
Unannounced
Availability Codes
and/or
A-1

DTIC COPY INSPECTED

FIGURES

TABLES

PREVIOUS PAGE IS BLANK

I. INTRODUCTION

Solar coronal plasmas have temperatures in the range of approximately 1×10^6 K (outside active regions) to 3×10^7 K (hot thermal flares). The X-ray line spectrum from these plasmas is rich and provides a means for analyzing the thermodynamic properties of the plasmas. The flare spectrum is most complex in the range 12-16 Å, where emission from Fe XVII-XXI dominates. At longer wavelengths the spectrum is not so rich, but over 60 lines have been identified in the range 15.5-23.0 Å (McKenzie and Landecker 1982a). The spectrum shortward of 12 Å includes the strongest lines of Fe XXII-XXIV, which are important for flare temperature analysis, and a surprising number of unidentified lines. This wavelength range was included in the spectrum analyzed by Phillips _et al._ (1982), but their long spectral scan (17.5 minutes) started after the flare peak. Consequently, many of the lines reported here were not observed by these authors.

Since their launch aboard the U.S. Air Force P78-1 satellite in 1979 February, the SOLEX collimated Bragg crystal spectrometers have obtained a large number of 3-23 Å X-ray spectra of solar active regions and flares. In this report we treat the line emission in the 5.5-12 Å range. We observed only a few relatively weak lines short of this range, and the predominantly Fe spectrum at longer wavelengths has been amply discussed from both theoretical and observational viewpoints.

PREVIOUS PAGE IS BLANK

In Section II we present the spectral data and the line identifications. A significant fraction of the lines remain unidentified; but, in some cases, the use of spectra representative of nonflaring, flaring, and post-flare conditions allows us to narrow the range of possible emitting species. In Section III we discuss the iron line spectra in detail. Section IV treats the line ratios from the helium-like species Mg XI, Al XII, and Si XIII. We have previously presented similar data for O VII and Ne IX (McKenzie and Landecker 1982b).

II. LINE SPECTRA

A. OBSERVATIONS

The spectrometers have been described by Landecker, McKenzie, and Rugge (1979). There were two collimated spectrometer systems: a 20-arc-second square collimator with a proportional counter detector (SOLEX A) and a 60-arc-second square collimator with a channel-electron-multiplier array (CEMA) detector (SOLEX B). Each spectrometer system employed either an ammonium dihydrogen phosphate (ADP) or a rubidium acid phthalate (RAP) crystal. In effect, there were four available spectrometers, but only two could be used at any one time. For the measurements described here, we used three: SOLEX A ADP (5.5-9.4 Å), SOLEX B RAP (7.8-12.0 Å), and SOLEX B ADP (5.5-9.2 Å).

The observed lines are tabulated in Table 1. Spectra of the following flares were examined: 1979 March 31, 17:07 UT, S24,E21; 1979 March 31, 23:21 UT, S24,E19 (McKenzie and Landecker 1981); 1979 June 5, 05:14 UT, N20,E17; 1980 April 8, 03:07 UT, N12,W10; and 1981 May 5, 14:09 UT, N16,E01. Nonflare spectra from Active Region 1661 (McMath Plage System 15918), taken at ~ 11:00 UT on 1979 March 31, ~ 11:00 UT, on 1979 April 3, and ~ 00:00 UT on 1979 April 5, were included as examples of spectra from lower-temperature plasmas. For each of these three observations, approximately ten successive spectral scans were summed in order

Table 1. Spectral Lines

λ_{obs}(Å)		Transition	λ_{ref}(Å)	Ref[h]	Strength[i]	Comment
5.683	Si XIII	$1s^2\ ^1S_0 - 1s3p\ ^1P_1$	5.680	8	0.02	...
6.184	Si XIV	$1s\ ^2S_{1/2} - 2p\ ^2P$	6.182	12	0.14	...
6.646	Si XIII	$1s^2\ ^1S_0 - 1s2p\ ^1P_1$	6.646	8	0.24	...
6.659	Si XII	$1s^23k\ ^2K - 1s2p3k\ ^2K'$	6.655	20	...	...
6.686	Si XIII	$1s^2\ ^1S_0 - 1s2p\ ^3P$	6.688	8	0.04	...
6.692	Si XII	$1s^22s\ ^2S_{1/2} - 1s2p(^3P)2s\ ^2P$ (st)	6.689	11	...	...
6.720	Si XII	$1s^22s\ ^2S_{1/2} - 1s2p(^1P)2s\ ^2P$ (qr)	6.719	11	...	...
6.738	Si XIII	$1s^2\ ^1S_0 - 1s2s\ ^3S_1$	6.740	8	0.10	...
7.107	Mg XII	$1s\ ^2S_{1/2} - 3p\ ^2P$	7.106	12	0.08	...
7.170	Al XIII	$1s\ ^2S_{1/2} - 2p\ ^2P$	7.173	12	0.04	...
7.477	Mg XI	$1s^2\ ^1S_0 - 1s4p\ ^1P_1$	7.473	8	0.05	...
7.685		Fe	7.680	2	0.03	a
7.761	Al XII	$1s^2\ ^1S_0 - 1s2p\ ^1P_1$	7.757	8	0.06	...
7.779	Al XI	$1s^23k\ ^2K - 1s3k2p\ ^2K'$	7.770	20	...	b
7.810	Al XII	$1s^2\ ^1S_0 - 1s2p\ ^3P$	7.807	8	0.02	...
7.854	Mg XI	$1s^2\ ^1S_0 - 1s3p\ ^1P_1$	7.850	8	0.08	...
7.875	Al XII	$1s^2\ ^1S_0 - 1s2s\ ^3S_1$	7.872	8	0.04	...
7.952		...	...	...	...	b
7.989	Fe XXIV	$2s\ ^2S_{1/2} - 4p\ ^2P_{3/2}$	7.983	7,2	0.05	a
7.999	Fe XXIV	$2s\ ^2S_{1/2} - 4p\ ^2P_{1/2}$	7.993	7,2	0.03	a
8.141		...	...	...	(0.01)	b
8.153		Fe	...	2	0.05	a
8.233	Fe XXIV	$2s\ ^2S_{1/2} - 4d\ ^2D_{3/2}$	8.231	7,2	0.05	a
8.305	Fe XXIII	$2s^2\ ^1S_0 - 2s4p\ ^1P_1$	8.307	7,19	0.08	...

Table 1. Spectral Lines (Continued)

λ_{obs}(Å)		Transition	λ_{ref}(Å)	Ref[h]	Strength[i]	Comment
8.318	Fe XXIV	$2p\ ^2P_{3/2} - 4d\ ^2D$	8.315	7,2	0.06	a
8.376	Fe XXIV	$2p\ ^2P_{3/2} - 4s\ ^2S_{1/2}$	8.371	7,2	0.05	a
8.421	Mg XII	$1s\ ^2S_{1/2} - 2p\ ^2P$	8.421	12	0.55	c
8.574		Fe	8.575	2	0.05	...
8.619		Fe	8.614	2	(0.01)	...
8.811	Fe XXIII	$2s2p\ ^1P_1 - 2s4d\ ^1D_2$	8.814	10	0.09	a
8.920		...	...	...	(0.03)	b
8.975	Na X	$1s^2\ ^1S_0 - 1s4p\ ^1P_1$	8.983	8	0.15	...
	Fe XXII	$2s^22p\ ^2P_{1/2} - 2s^24d\ ^2D_{3/2}$	8.98	17,16		
9.074		Fe	9.073	2	0.12	...
9.114		Fe	9.110	2	(0.02)	b
9.169	Mg XI	$1s^2\ ^1S_0 - 1s2p\ ^1P_1$	9.169	8	1.00	c
9.182	Mg X	$1s^24k\ ^2K - 1s2p4k\ ^2K'$	9.180	18	...	...
9.196	Mg X	$1s^23k\ ^2K - 1s2p3k\ ^2K'$	9.193	18	(0.04)	...
9.231	Mg XI	$1s^2\ ^1S_0 - 1s2p\ ^3P$	9.231	8	0.18	c
9.241	Mg X	$1s^22s\ ^2S_{1/2} - 1s2p(^3P)2s\ ^2P$ (st)	9.236	11	...	b
9.289	Mg X	$1s^22s\ ^2S_{1/2} - 1s2p(^1P)2s\ ^2P$ (qr)	9.284	11	...	b
9.314	Mg XI	$1s^2\ ^1S_0 - 1s2s\ ^3S_1$	9.314	8	0.46	c
9.322	Mg X	$1s^22p\ ^2P_{3/2} - 1s2p^2\ ^2D_{5/2}$ (j)	9.321	11	...	...
		$1s^22p\ ^2P_{1/2} - 1s2p^2\ ^2D_{3/2}$ (k)	9.318			
9.390		...	9.389	2	...	...
9.479	Ne X	$1s\ ^2S_{1/2} - 5p\ ^2P$	9.481	12	0.28	...
9.525		...	...	...	0.11	a
9.554		...	...	...	0.21	a
9.585		...	...	...	0.20	a

Table 1. Spectral Lines (Continued)

λ_{obs}(Å)		Transition	λ_{ref}(Å)	Ref[h]	Strength[i]	Comment
9.656		...	...	...	0.10	a
9.717	Ne X	1s $^2S_{1/2}$ - 4p ^2P	9.708	12	0.25	...
9.810		...	...	...	...	...
9.858		...	...	...	...	...
9.902		...	...	...	...	b
10.000 / 10.069		Fe(XX?)	9.996	2,3	0.41	e
	Na XI	1s $^2S_{1/2}$ - 2p ^2P	10.025	12		
		Fe(XX?)	10.065	2,3		
10.133		...	10.128	2	0.24	...
		...	10.134	2		
10.245	Ne X	1s $^2S_{1/2}$ - 3p ^2P	10.239	12	0.32	c
10.328		...	...	...	0.18	a
10.359		Fe	10.354	2,6	0.27	...
10.502	Fe XVII	$2p^6$ $^1S_0$ - $2p^5 7d$ $^3D_1$	10.500	15	(0.14)	c
10.530		...	...	...	...	...
10.577	Fe XIX	$2p^4$ $^3P_1$ - $2p^3(^2P)4d$ $^3D_2$	10.572	5,2,6	0.12	...
	Fe XIX	$2p^4$ $^3P_1$ - $2p^3(^2P)4d$ $^3P_1$	10.583	5,2,6		
10.612	Fe XXIV	2s $^2S_{1/2}$ - 3p $^2P_{3/2}$	10.612	14	1.28	a
10.647	Ne IX	$1s^2$ $^1S_0$ - 1s6p $^1P_1$	10.646	8	(0.34)	d,f
10.654	Fe XXIV	2s $^2S_{1/2}$ - 3p $^2P_{1/2}$	10.654	14	0.81	a
10.769	Fe XVII	$2p^6$ $^1S_0$ - $2p^5 6d$ $^3D_1$	10.768	15	0.33	c
	Ne IX	$1s^2$ $^1S_0$ - 1s5p $^1P_1$	10.764	8		
10.821	Fe XIX	$2p^4$ $^3P_2$ - $2p^3(^4S)4d$ $^3D_3$	10.813	3	0.43	...
	Ni XXII	$2p^3$ $^4S_{3/2}$ - $2p^2 3d$ $^4P_{5/2,3/2}$	10.83	9		

Table 2. Lines of Fe XXIII (n = 3-2)

Transition	Wavelength Calc.	Wavelength Obs.	Strength Calc.	Strength Obs.
$2s^2\ {}^1S_0 - 2s3p\ {}^1P_1$	10.980	10.977	1.00	1.00
$2s^2\ {}^1S_0 - 2s3p\ {}^3P_1$	11.018	11.025	0.72	1.60[a]
$2s2p\ {}^3P_0 - 2s3d\ {}^3D_1$	11.325	---	0.05	---
$2s2p\ {}^3P_1 - 2s3d\ {}^3D_1$	11.361	---	0.04	---
$2s2p\ {}^3P_2 - 2s3d\ {}^3D_3$	11.459	---	0.19	---
$2s2p\ {}^3P_2 - 2s3d\ {}^3D_2$	11.485	11.493	0.04	0.18
$2s2p\ {}^1P_1 - 2s3d\ {}^1D_2$	11.737	11.739	1.91	2.04
$2s2p\ {}^1P_1 - 2s3s\ {}^1S_0$	12.15	12.196	1.32	0.48

[a]Blend with Fe XXIV; see §IIIc.

The Fe XXIII line strengths for the n = 3-2 transitions have been calculated by Bhatia and Mason (1981; hereafter, BM). Table 2 lists Fe XXIII transitions along with theoretical (BM) and observed line strengths relative to the $2s^2\ ^1S_0 - 2s3p\ ^1P_1$ line at 10.977 Å for the 1981 May 5 spectrum shown in Figure 1. Figure 2 indicates that the contamination of this line by low-temperature emission is relatively small; compare with the two "cool" lines around 10.8 Å. In addition to the lines in Table 1, we include the $2s2p\ ^1P_1 - 2s3s\ ^1S_0$ line predicted at 12.15 Å, slightly outside the spectral range treated in this report (the data for this line are also from the 1981 May 5 spectrum). BM suggest that a line observed at 12.198 Å in an earlier SOLEX spectrum (McKenzie et al. 1980b) might correspond to this line, or that the line might be blended with the very strong Fe XVII and Ne X lines at 12.127 Å. In the spectra under discussion here, we find a line at 12.196 Å, and its emission as a function of temperature is consistent with its being from Fe XXIII. The possibility of a blend around 12.13 Å cannot be ruled out.

Table 2 shows that theory and experiment are in good agreement with regard to the strong line at 11.739 Å. The line at 11.025 Å is a blend with Fe XXIV, and Figure 2 indicates that there is a contribution from low-temperature emission as well. Table 3 in §IIId indicates that the flux is only adequate to account for the predicted Fe XXIV emission alone. Since the line

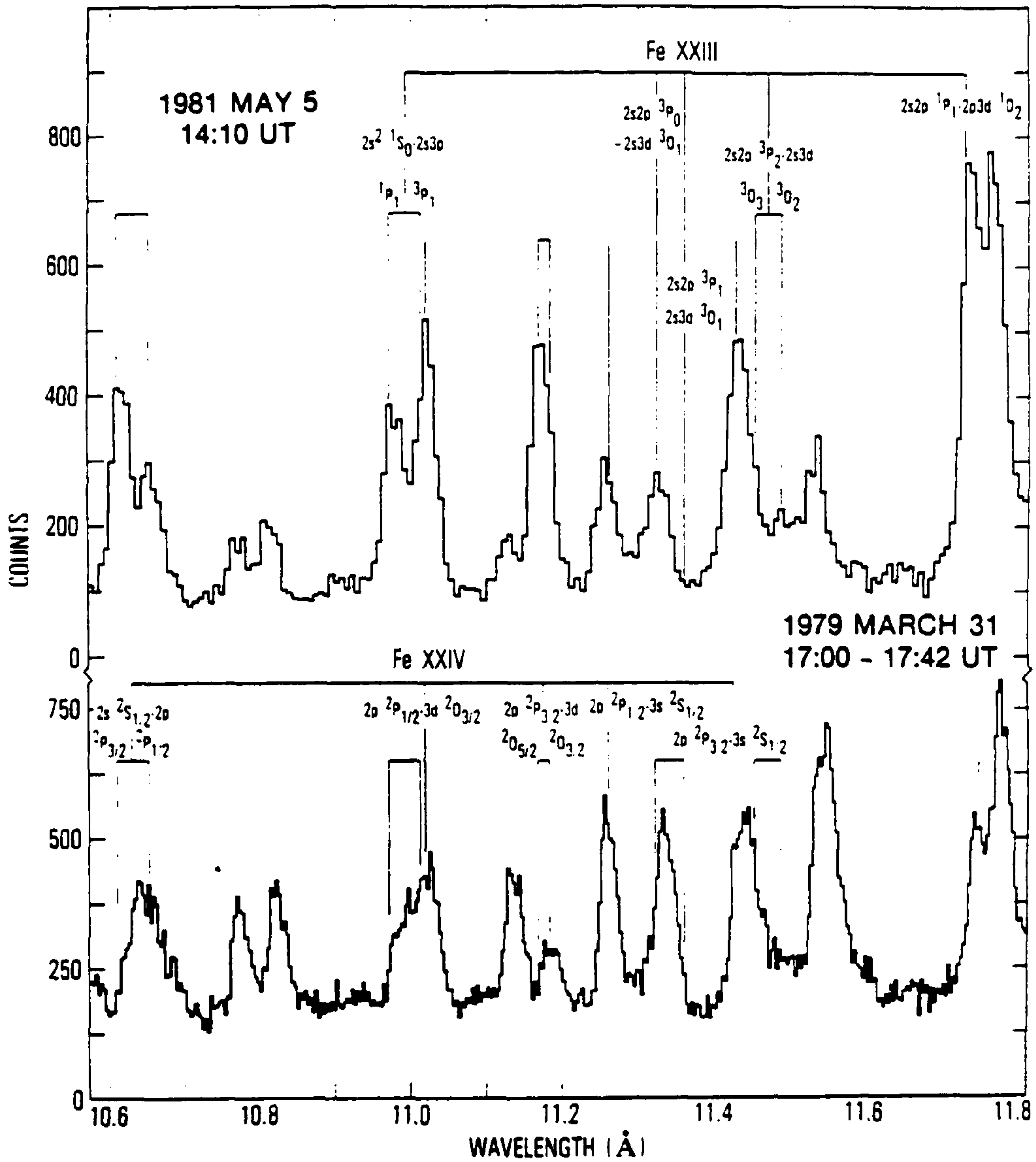

Figure 2. Two SOLEX B RAP spectra showing the n = 3-2 Fe XXIII and Fe XXIV transitions. The fiducial marks indicate the calculated wavelengths of the Fe XXIII and XXIV lines. The upper spectrum was taken at 14:10 UT on 1981 May 5, at the onset of a solar flare. The spectrometer scanning rate was 0°.525 s^{-1}. The lower spectrum is the sum of ten scans between 17:00 UT and 17:42 UT on 1979 March 31. The scanning rate was 0°.262 s^{-1}. Most of the Fe XXIII and XXIV lines were obscured by "cooler" lines in the latter spectrum.

flare onset; hence they probably arise from a region at high temperature. The laser plasma iron spectrum reported by Boiko, Faenov, and Pikuz (1978) lists a number of lines in this wavelength range. The observed lines may arise from n = 4 - 2 Fe XXII transitions.

C. LINES OF Fe XXIII

The attribution of spectral lines to Fe XXIII and Fe XXIV can be done with confidence because the lines are strong in high-temperature ($\gtrsim 10^7$ K) plasmas. The only identified lines in Table 1 that are observed (and resolved) only in *flare-onset spectra* come from these two species. It is therefore probable that the unidentified lines at 8.153 Å and 7.685 Å come from Fe XXIII or XXIV and that the one at 9.114 is a weak line from a lower Fe ionization stage. Figure 2 presents plots of the Fe XXIII and XXIV spectra under different temperature conditions: the flare onset spectrum at 14:10 UT on 1981 May 5 and the sum spectrum for the flare at 17:07 UT on 1979 March 31. The wavelengths of the n = 3-2 transitions of Fe XXIII and Fe XXIV are shown. The lines at 10.769 Å (Fe XVII, 5×10^6 K, and Ne IX, 4×10^6 K), 10.821 Å (Fe XIX, 7×10^6 K, and Ni XXII, 8×10^6 K), and 11.544 Å (Fe XVIII, 6×10^6 K, and Ne IX, 4×10^6 K) can be used as indicators of the emissions from lower-temperature plasmas. The temperature estimates are based on ionization equilibrium calculations by Jacobs et al. (1977, 1980).

be blended with the Na X line briefly mentioned in Section II. We accept this identification. It is likely that Fe XXII dominates the blend in the SOLEX spectra, since the calculated line strength, based on our measurements of the 11.773-Å line and Mason and Storey's calculated ratio, is 0.20 times the Mg XI 9.169-Å line strength. The normalized strength in Table 1 is 0.15.

The line at 11.932 Å is identified as $2s^22p\ ^2P_{3/2}$ - $2s^23d\ ^2D_{3/2,5/2}$, with the J = 3/2 line dominant, in accordance with MS for plasmas of density $\lesssim 10^{12}$ cm^{-3}. The wavelength in MS does not agree with the observed value; in fact the agreement between the calculated wavelengths in MS and the observed solar wavelengths is poor for all four lines discussed here. By using wavelengths of 845.1 Å (Mori, Otsuka, and Kato 1979) for the $2s^22p\ ^2P_{1/2}$ - $2s^22p\ ^2P_{3/2}$ transition and 11.773 Å (our value) for the $2s^22p\ ^2P_{1/2}$ - $2s^23d\ ^2D_{3/2}$ transition, we calculate a wavelength of 11.939 Å for the $2s^22p\ ^2P_{3/2}$ - $2s^23d\ ^2D_{3/2}$ transition, in agreement with Neupert, Swartz, and Kastner (1973). With the upper-level splitting in MS, the wavelength for $2s^22p\ ^2P_{3/2}$ - $2s^23d\ ^2D_{5/2}$ is 11.925 Å. For the line at 11.882 Å we follow Boiko, Faenov, and Pikuz (1978) in accepting the identification by Fawcett and Hayes (1975). MS does not provide data for the 2s2p3d configuration.

Table 1 includes four unidentified lines in the wavelength range 9.5 - 9.7 Å. Each of these lines was observed only near

III. LINES OF Fe XXII - XXIV

A. INTRODUCTION

The lines of Fe XXII - XXIV are particularly interesting because of their applicability in the analysis of hot flare plasmas. Recent papers by Mason and Storey (1980), Bhatia and Mason (1981), and Hayes (1979) allow us to compare measured relative line strengths from each stage of ionization with theory. The spectra summarized in Table 1 include transitions of the form $2\ell - n\ell'$ for n = 3 and 4 for all three species. In this section we discuss those lines.

B. LINES OF Fe XXII

Table 1 includes four lines from Fe XXII. By far the strongest is the 2p $^2P_{1/2}$ - 3d $^2D_{3/2}$ line at 11.773 Å. With the calculations by Mason and Storey (1980; hereafter, MS), this is a valuable temperature diagnostic line. In the SOLEX spectra it is partially blended with, but easily separable from, the Fe XXIII 2s2p $^1P_1$ - 2s3d $^1D_2$ line at 11.737 Å.

MS give 8.920 Å as the wavelength for the $2s^22p$ $^2P_{1/2}$ - $2s^24d$ $^2D_{3/2}$ line. The SOLEX line at this wavelength is only 1% as strong as the 11.773-Å line, whereas MS predict a ratio of 0.09 for the two lines. Neupert, Swartz, and Kastner (1973) assign a wavelength of 8.98 Å to the line under discussion; thus it would

The 8.975 Å line is too strong to be attributed solely to the Na X transition noted. A probable Fe XXII blend will be discussed in Section III. The line at 9.390 Å corresponds well in wavelength to the Ni XXVI 2p $^2P_{1/2}$ - 3d $^2D_{3/2}$ line, but the 2p $^2P_{3/2}$ - 3d $^2D_{5/2}$ line, at 9.535 Å (Fawcett, Ridgeley, and Hughes 1979), is not observed. In Fe XXIV these lines are of comparable strength. Furthermore, the 9.390 Å line is just as strong relative to the Ne IX line at 9.479 Å in the flare sum as it is in the onset spectrum; it is not a "hot" line. For these reasons we do not adopt the Ni XXVI identification. The only Ni lines we identify are at 10.821 and 11.834 Å. The Ni XXII lines at 10.821 Å arise from the same transitions that produce the strongest Fe XX lines (Mason and Bhatia 1983). The line at 11.025 Å is observed in nonflaring active regions that are much too cool to produce Fe XXIII and Fe XXIV emission. Therefore, although the Fe XXIII and Fe XXIV emissions are strong near the flare peak, there must be an additional line near 11.025 Å that arises from an ionic species present at temperatures below ~ 5 x 10^6 K. Swartz et al. (1971) attributed a laboratory-measured line at 11.021 Å to Fe XVIII $2p^5\ ^2P_{3/2} - 2p^4(^1S)4d\ ^2D_{5/2}$.

two measurements agree as well as they do indicates that the fluxes are probably not grossly underestimated.

B. DISCUSSION OF SELECTED LINES

A number of lines in Table 1 require further discussion or clarification. The following paragraphs provide that discussion. The lines of Fe XXII - XXIV will be discussed in § III.

Boiko, Faenov, and Pikuz (1978) presented an extensive list of Fe L lines observed in a laser plasma. Their list includes nearly 300 lines in the wavelength range being discussed here. It contains unidentified lines having wavelengths near several of the unidentified lines in Table 1; see the reference column. The line at 10.000 Å, the strongest of the blended lines in this region, and the one at 10.069 Å are identified on the strength of calculations by Bromage et al. (1977a) and observations by Boiko, Faenov, and Pikuz. The lines at 10.359 Å and 10.530 Å may arise from $2p^4 5d$ levels of Fe XVIII (Bromage et al. 1977a). The line at 10.577 Å corresponds well to calculated wavelengths for the two listed Fe XIX lines (Bromage, Fawcett, and Cowan 1977b), and Boiko, Faenov, and Pikuz (1978) observed lines near the calculated wavelengths. Finally, Boiko, Faenov, and Pikuz observed a relatively strong unidentified line at 11.976 Å.

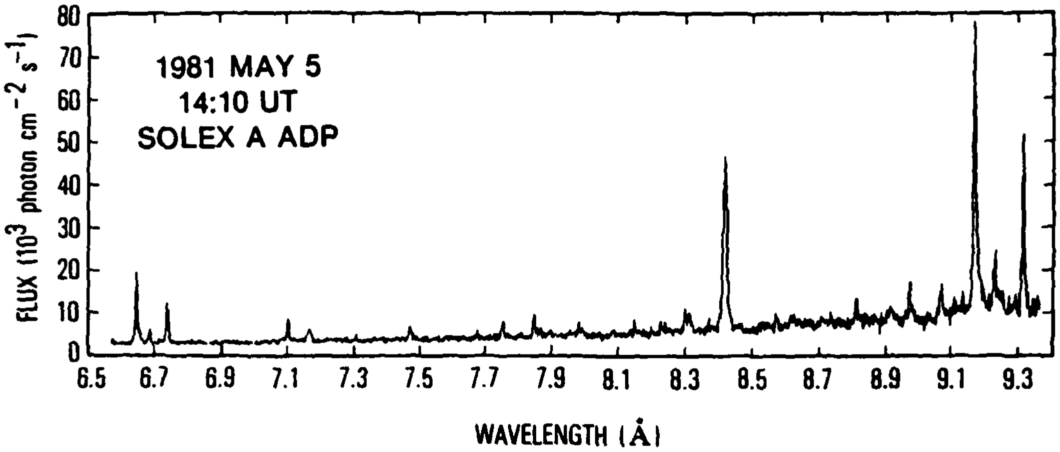

Figure 1A.

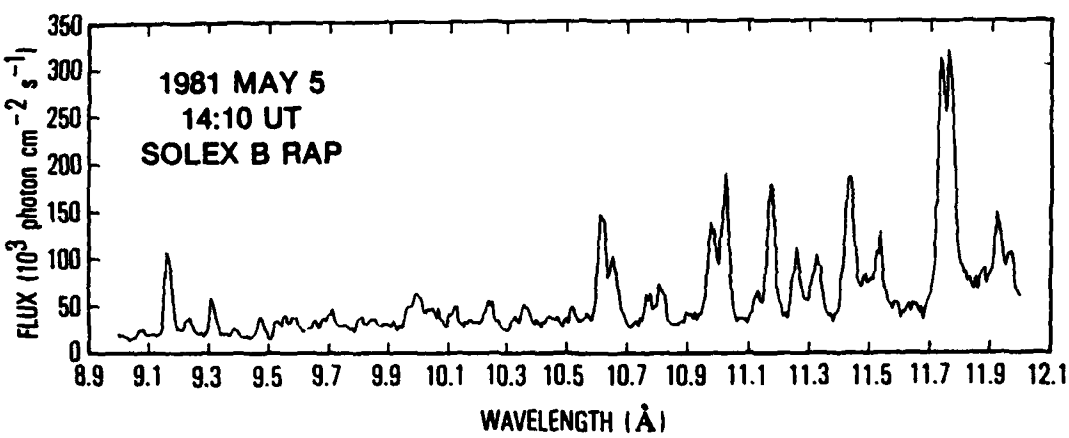

Figure 1B.

Figure 1. The X-ray emission-line spectrum taken near the onset of a solar flare. The calibration is such that the flux from a spectral line corresponds to the peak value in the plot. Two spectrometers were used in measuring the spectrum, and, for comparison, the plots overlap in the range 9.0 to 9.3 Å.

Figures 1a and 1b show the spectrum observed near the onset and peak of the 1981 May 5 flare. This spectrum is particularly rich in lines from species present at high temperatures (greater than 10^7 K). Omitting the range from 5.5 - 6.5 Å from figure 1a permits a substantially larger-scale presentation with only two of the detected lines not shown. Although the spectral scan depicted took 84 seconds to accumulate (14:09:23 - 14:10:47 UT), variations in line flux were relatively small during this time period. For example, the Mg XI 9.169 Å line flux increased by 10% between 14:09:28 and 14:12:09, and the Fe XXIII 11.737 Å line flux decreased by 25% between 14:09:40 and 14:11:53 UT. The ordinates on the figures show absolute fluxes, and the plots are calibrated such that the total flux in a given line can be read from the line's peak; it is not necessary to integrate over the line profile. The calibration assumes that the radiation comes from a point source centered in the collimator's field of view. Since this assumption is certainly violated to some extent, the fluxes in the figures are lower limits. It should be noted that the flux for the Mg XI line at 9.169 Å as measured by SOLEX B is ~ 1.5 times that measured by SOLEX A. This can be explained by the fact that the two spectrometers do not have a common field of view. SOLEX A has a 20-arc-second field of view, and SOLEX B has a 60-arc-second field of view. Furthermore, there is a pointing offset of 31 arc seconds between the two collimators. The fact that the

The fifth column gives the line strength as the flux normalized to that measured in the Mg XI $1s^2\ ^1S_0 - 1s2p\ ^1P_1$ line. This reference line is scanned by each of the three spectrometers for which we are presenting measurements here. Thus each line strength can be normalized to a flux measured by the same spectrometer used in the measurement of that line. The relative line strengths are measurements at 14:09 - 14:11 UT on 1981 May 5, at the onset of that flare. Thus they are typical of a relatively hot flare plasma. The strengths are based on the counting rates at the peak of the lines. Except where weak or blended lines are concerned, the relative strengths are estimated to be accurate to ~ 20%. A few of the lines were obscured or weak in the 1981 May 5 spectrum, so their relative fluxes are for a summed series of ten scans during the 1979 March 31, 17:07 UT flare. These strengths are in parentheses. The lines for which no strengths are given are either weak lines blended with much stronger ones or not observed in flares.

The last column in the table is for comments. Lines for which this column is blank were observed under all flare conditions but not in nonflaring active regions (few nonflare spectra are available for $\lambda < 7.8$ Å). Lines prominent only near flare onset are noted; in many cases, they were obscured by other lines as the flare plasma cooled. A few weak lines were only detectable by summing several spectra. Finally, those lines observed in the nonflare spectra are noted.

to improve line-detection sensitivity. The summing technique was also used on the earlier 1979 March 31 flare and on the 1981 May 5 flare, and all flare spectra were examined individually so that the evolution of the line emission could be observed.

The first column of the table gives the wavelength and the second the line identification. Of the 85 lines in the table, 22 cannot be identified with confidence. For the satellite lines from lithium-like ions, the letter designations in Gabriel's (1972) nomenclature are given in parentheses. The wavelengths were determined by first finding the spectrometer step number at the centroid of the line. This step number was converted by using an analytical formula relating it to wavelength. A final small correction to the formula was made by using very well determined wavelengths of strong lines as benchmarks. At wavelengths below 9.35 Å, where ADP spectra were available, the accuracy is estimated to be 3 mÅ. At longer wavelengths, where the lower-dispersion RAP spectra were used, the estimated accuracy is 5 mÅ.

The third and fourth columns give previously determined wavelengths for the lines and the references from which the wavelengths are drawn. In selecting references we gave first priority to recent calculations and second priority to laboratory experiments with well-defined plasmas. In the absence of these sources, solar spectra were used.

Table 1. Spectral Lines (Continued)

a) Observed in flare onset only

b) Observed in flare sum only

c) Also, observed in nonflaring active region

d) Observed in nonflaring active region and flare sum only

e) Blend of more than 2 lines

f) Blend, centroid wavelength listed

g) Resolved in nonflaring active region only

h) REFERENCES - (1) Bhatia and Mason 1981. (2) Boiko et al. 1978. (3) Bromage et al. 1977a. (4) Bromage et al. 1978. (5) Bromage et al. 1977b. (6) Cohen and Feldman 1970. (7) Doschek, Meekins, and Cowan 1972. (8) Ermolaev and Jones 1973. (9) Fawcett and Hayes 1975. (10) Fawcett et al. 1979. (11) Gabriel 1972. (12) Garcia and Mack 1965. (13) Gordon et al. 1980. (14) Hayes 1979. (15) Hutcheon et al. 1976. (16) Mason and Storey 1980. (17) Neupert et al. 1973. (18) Parkinson 1975. (19) Reader and Sugar 1975. (20) Calculated from Summers 1973. (21) Swartz et al. 1971.

i) Relative to Mg XI 9.169 A; see text.

Table 1. Spectral Lines (Continued)

λ_{obs}(Å)	Transition		λ_{ref}(Å)	Ref[h]	Strength[i]	Comment
10.977	Fe XXIII	$2s^2\ ^1S_0 - 2s3p\ ^1P_1$	10.980	1	1.07	a
10.994	Ne IX	$1s^2\ ^1S_0 - 1s4p\ ^1P_1$	11.000	8	(0.11)	d
	Na X	$1s^2\ ^1S_0 - 1s2p\ ^1P_1$	11.003	8		
11.025	Fe XXIV	$2p\ ^2P_{1/2} - 3d\ ^2D_{3/2}$	11.025	14	1.60	c
	Fe XXIII	$2s^2\ ^1S_0 - 2s3p\ ^3P_1$	11.018	1		
	Fe XVIII	$2p^5\ ^2P_{3/2} - 2p^4(^1S)4d\ ^2D_{5/2}$	11.021	21		
11.129	Fe XVII	$2p^6\ ^1S_0 - 2p^5 5d\ ^1P_1$	11.129	15	0.36	c
11.170	Fe XXIV	$2p\ ^2P_{3/2} - 3d\ ^2D_{5/2}$	11.166	14	1.56	a
11.187	Na X	$1s^2\ ^1S_0 - 1s2s\ ^3S_1$	11.192	8	(0.17)	b
11.256	Fe XVII	$2p^6\ ^1S_0 - 2p^5 5d\ ^3D_1$	11.250	15	0.85	c
11.332	Fe XVIII	$2p^5\ ^2P_{3/2}$	11.325	5	0.67	c
		$2p^4(^1D)4d\ ^2F_{5/2},\ ^2P_{3/2},\ ^2S_{1/2}$				
11.428		...	...	...	...	g
11.431	Fe XXIV	$2p\ ^2P_{3/2} - 3s\ ^2S_{1/2}$	11.424	14	1.53	a
11.445	Fe XVIII	$2p^5\ ^2P_{1/2}$	11.440	5,6	(0.52)	d
		$2p^4(^1D)4d\ ^2P_{1/2},\ ^2D_{3/2}$				
11.493	Fe XXIII	$2s2p\ ^3P_2 - 2s3d\ ^3D_2$	11.485	1	0.19	a
11.544	Ne IX	$1s^2\ ^1S_0 - 1s3p\ ^1P_1$	11.547	8	0.84	c
	Fe XVIII	$2p^5\ ^2P_{1/2} - 2p^4(^3P)4d\ ^2P_{3/2}$	11.551	13		
11.739	Fe XXIII	$2s2p\ ^1P_1 - 2s3d\ ^1D_2$	11.737	1	2.18	...
11.773	Fe XXII	$2p\ ^2P_{1/2} - 3d\ ^2D_{3/2}$	11.767	4	2.27	...
11.834	Ni XX	$2p^5\ ^2P_{3/2} - 2p^4(^1D)3d\ ^2D_{5/2}$	11.832	13	(0.13)	b
11.882	Fe XXII	$2s2p^2\ ^4P_{5/2} - 2s2p(^3P)3d\ ^4P_{5/2}$	11.886	2,9	0.22	...
11.932	Fe XXII	$2s^2 2p\ ^2P_{3/2} - 2s^2 3d\ ^2D_{3/2,5/2}$	11.94	17	0.94	...
11.970		Fe	11.976	2	0.41	...

Table 3. Lines of Fe XXIV (n = 3-2)

Transition	Wavelength Calc.	Wavelength Obs.	Strength Calc.	Strength Obs.
$2s\ ^2S_{1/2} - 3p\ ^2P_{3/2}$	10.612	10.612	1.00	1.00
$2s\ ^2S_{1/2} - 3p\ ^2P_{1/2}$	10.654	10.654	0.53	0.63
$2p\ ^2P_{1/2} - 3d\ ^2D_{3/2}$	11.025	11.025	1.28	1.25[a]
$2p\ ^2P_{3/2} - 3d\ ^2D_{5/2}$	11.166	11.170	2.34	1.22
$2p\ ^2P_{3/2} - 3d\ ^2D_{3/2}$	11.181	---	0.27	---
$2p\ ^2P_{1/2} - 3s\ ^2S_{1/2}$	11.262	---	0.53	---
$2p\ ^2P_{3/2} - 3s\ ^2S_{1/2}$	11.424	11.431	1.22	1.20

[a]Blend with Fe XXIII; see § IIIc

is observed at the Fe XXIV wavelength, it appears that Fe XXIV dominates the blend but that the fluxes of both high-temperature lines fall short of prediction. Although we observe a line near 11.325 Å, this cannot be attributed to Fe XXIII because its emission varies with temperature in the same manner as does that of the low-temperature lines in Figure 2. The flux for the Fe XXIII line is expected to be low; similar to that of the line at 11.361 Å, which is not detected. The flux indicated for the line at 11.493 Å is larger than expected. The difficulty of making a background estimate for this line can be appreciated by examining Figure 2. The flux uncertainty is large. The line at 12.196 Å is weaker than BM predicted the 2s2p $^1P_1$ - 2s3s $^1S_0$ line to be, and this casts some doubt on the identification. Again, the Fe XXIII line could be obscured by a blend at 12.127 Å.

Two Fe XXIII n = 4-2 transitions are detected at 8.305 and 8.811 Å. The lines are of approximately equal strength, and neither is blended. Though relatively weak, the lines might be useful in temperature analysis.

D. LINES OF Fe XXIV

Table 1 includes five n = 3-2 and five n = 4-2 Fe XXIV lines. Hayes (1979) has provided data from which the relative strengths of the n = 3-2 lines can be computed. We have computed the strengths for a temperature of 1.5×10^7 K. The calculated and observed line strengths are given in Table 3. Again, the 1981 May 5 flare-onset spectrum is used. The line strengths are normalized to the $2s^2\ ^2S_{1/2}$ - $2s3p\ ^2P_{3/2}$ line at 10.612 Å, a line that has only minor contamination from low-temperature emission. The agreement between theory and experiment is good for the lines at 10.654 and 11.424 Å. Both are blended with low-temperature lines which make some contribution to their apparent emissions, so their fluxes are slightly below the predicted values. As discussed in §IIIc, the line at 11.025 Å is probably also weaker than it is calculated to be. The major surprise is the relative weakness of the $2p\ ^2P_{3/2}$ - $3d\ ^2D_{5/2}$ line. The observed line has only very minor contributions from low-temperature emissions and the $2p\ ^2P_{3/2}$ - $3d\ ^2D_{3/2}$ line. The expected line at 11.262 Å is weak compared to low-temperature emissions near that wavelength.

Five Fe XXIV n = 4-2 lines, including the $2p\ ^2P_{3/2}$ - $4d\ ^2D_{5/2,3/2}$ blend, were observed. Of the n = 4-2 transitions identified by Boiko, Faenov, and Pikuz (1978), only the $2p\ ^2P_{1/2}$ - $4s\ ^2S_{1/2}$ line, expected at 8.285 Å, was undetected. The corresponding n = 3-2 transition is predicted to be relatively weak (Hayes 1979) and was not resolved in the SOLEX spectra. Each of the n=4-2 lines was detected only in the flare-onset spectrum, and with the exception of the blend mentioned above, each was well resolved. In view of the blends with the n = 3-2 transitions, the n = 4-2 transitions could be useful diagnostically if theoretical line strength calculations were available.

IV. LINES FROM HELIUM-LIKE IONS

Gabriel and Jordan (1969) first pointed out the potential usefulness as a measure of plasma density of the ratio R in the helium-like ions:

$$R = \frac{F(1s^2\ ^1S_0 - 1s2s\ ^3S_1)}{F(1s^2\ ^1S_0 - 1s2p\ ^3P)} , \qquad (1)$$

where F stands for "flux". So far, the O VII (McKenzie *et al.* 1980a; Doschek *et al.* 1981) and Ne IX (Wolfson *et al.* 1983) ratios have been used in density diagnosis. Acton and Brown (1978) studied the use of G,

$$G = \frac{F(1s^2\ ^1S_0 - 1s2s\ ^3S_1) + F(1s^2\ ^1S_0 - 1s2p\ ^3P)}{F(1s^2\ ^1S_0 - 1s2p\ ^1P_1)} , \qquad (2)$$

as an indicator of the state of ionization balance in the emitting plasma. The three transitions in equation 2 are conventionally called the resonance (^1P), intercombination (^3P), and forbidden (^3S) lines. Recent theoretical calculations of the line ratios have been made by Pradhan, Norcross, and Hummer (1981), Pradhan and Shull (1981), Pradhan (1982), Doyle, Tayal, and Kingston (1983), and Keenan, Tayal, and Kingston (1984). For O VII the agreement between theory and observation (McKenzie and Landecker 1982b) is excellent. Wolfson *et al.* (1983) presented theoretical

PREVIOUS PAGE IS BLANK

calculations as well as observational data for Mg XI and S XV in addition to Ne IX. In this section we present our results for Mg XI, Al XII, and Si XIII.

Although the Mg XI lines are routinely observed with SOLEX spectrometers using both RAP and ADP crystals, the RAP dispersion is small at short wavelengths, so the ADP measurements are better. In addition, the SOLEX B RAP spectrometer scans the O VII lines within 7 or 14 seconds (the spectrometer drive has two stepping rates) of the SOLEX A ADP scan over the Mg XI lines. This allows us to use the O VII measurements to monitor the electron density, albeit at a lower temperature of 2×10^6 K, while the Mg XI observations for $T = 6 \times 10^6$ K are being made. For the above reasons, we will discuss only the SOLEX A data for the flare of 1981 May 5.

The R ratio is related to the electron density n_e by (Gabriel and Jordan 1969)

$$n_e = n_0\left(\frac{R_0}{R} - 1\right) , \qquad (3)$$

where R_0 is the value R takes on in the low-density limit. Good spectroscopic measurements may be sensitive to densities as low as $n_e^* = n_0/10$, but imprecise knowledge of R_0 will raise this limit. For Mg XI, n_e^* is $\sim 10^{12}$ cm^{-3} (Pradhan 1982), which is of the same magnitude as the maximum densities measured using O VII

(Doschek et al. 1981) and Ne IX (Wolfson et al. 1983). The highest O VII density measured during the 1981 May 5 flare was ~ 1 x 10^{11} cm^{-3}. Although O VII and Mg XI are produced at different temperatures, the relatively low peak density at ~ 2 x 10^6 K makes it seem unlikely that the density at ~ 6 x 10^6 K exceeded n_e^* for Mg XI. Thus the R measurement is probably a determination of R_0.

Figure 3a shows the Mg XI spectrum summed over 18 scans for the May 5 flare. Satellite lines s,t,j, and k, in the notation of Gabriel (1972), can make significant contributions to the forbidden (F) or intercombination (I) line flux, and hence to the R ratio. We corrected for these lines by scaling from the measured strength of lines q and r using the data of Bhalla, Gabriel, and Presnyakov (1975) and assuming an electron and ion temperature of 6 x 10^6 K, the temperature of maximum Mg XI emission (T_m). The corrections reduced I and F fluxes by 8% and 6%, respectively. For the spectrum in Figure 3a we found R = 2.91 ± 0.28 and G = 0.75 ± 0.04. The R value is in agreement with both theoretical R_0 values and most experimental measurements (see compilations in Wolfson et al. 1983). The G ratio agrees with recent flare observations of Wolfson et al. 1983 and is lower than the value read off the plot in Pradhan (1982): ~ 0.9. Bromboszcz et al. (1983) have presented a plot relating G, R, T, and N_e, based on a careful theoretical analysis of all of the emission lines near the Mg XI lines (Siarkowski et al. 1982).

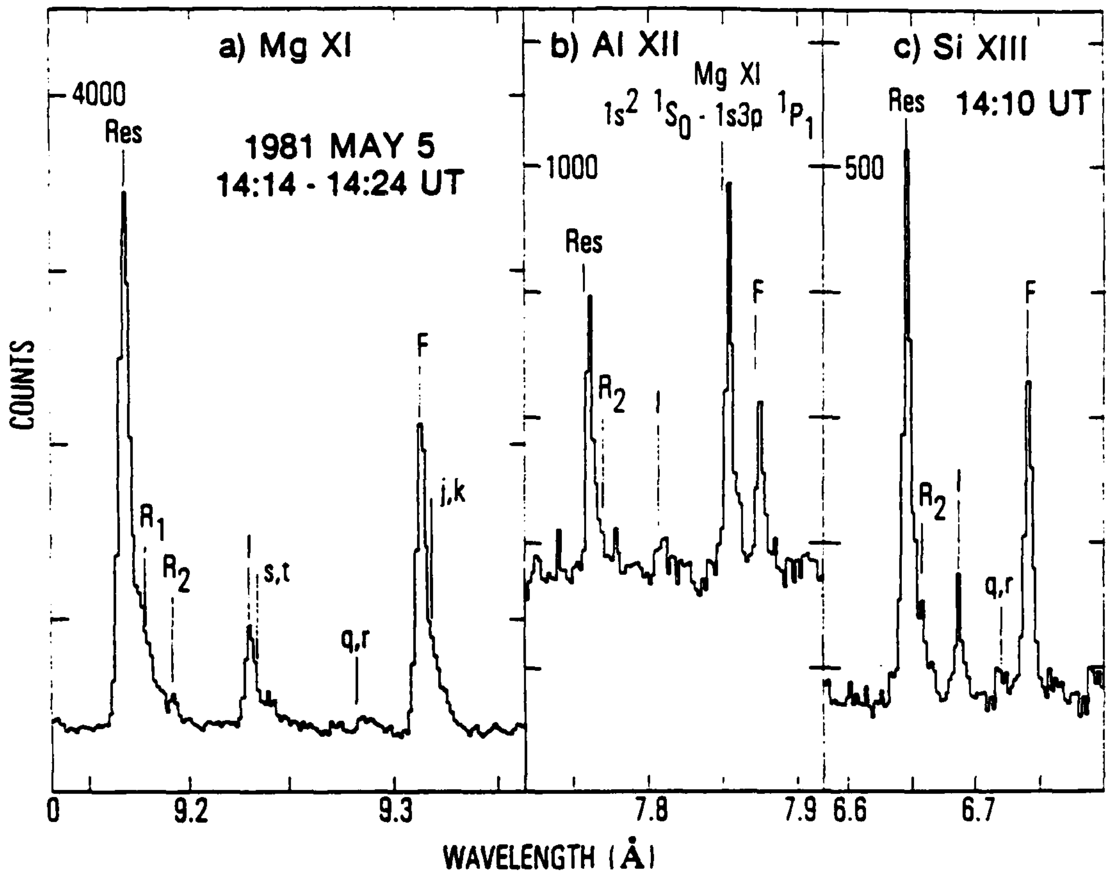

Figure 3. Lines of helium-like magnesium, aluminum, and silicon. The lines are marked at their calculated wavelengths. The vertical scales are different for the three segments; a reference number of counts is marked on each. Segments a) and b) are from the sum of 18 scans between 14:14 UT and 14:24 UT on 1981 May 5. Segment c) is a single scan at 14:10 UT. All of the data were taken with the SOLEX A ADP spectrometer.

Data from high-resolution spectra of a nonflaring active region are plotted on the same diagram (Krutov et al. 1981; Siarkowski et al. 1982). The plot does not extend to values of R and G as high as we observed, but an extrapolation would place our observed values at a position consistent with density below n_e^* and temperature around 7×10^6 K.

We also measured the ratios for the flare onset spectrum at 14:10 UT on 1981 May 5 and found R = 2.48 ± 0.37 and G = 0.64 ± 0.03. This lower value of R is marginally consistent with the value found from the flare sum. Figure 3a shows significant emission on the long-wavelength wing of I. Parkinson's (1975) active region spectrum also shows radiation longward of I, which he attributes to s and t or, in his terminology, I_2. However his I_2 is much weaker with respect to q and r (R_3) than is ours. Our relatively high emission may be partially attributable to unidentified iron line emission present at high temperature. Boiko, Faenov, and Pikuz (1978) list an unidentified line at 9.241 Å in their iron laser-plasma spectrum. Furthermore they list a line tentatively identified as Fe XXII $2s^22p\ ^2P_{3/2}$ - $2s^24s\ ^2S_{1/2}$ at 9.231 Å, the same wavelength as I. If this line exists, it could distort R determinations in high-temperature flare plasmas. R would increase as the flare cooled and the Fe XXII emission decreased. At the same time G would decrease, but this would be a small effect. In the present case, G was lower at the beginning of the flare when the temperature was high. This is in accord with the expected variation of G with temperature. Additionally, G might have been low because the plasma was in an ionizing state (Acton and Brown 1978).

The Al XII flare sum spectrum is shown in Figure 3b. The intrusion of a Mg XI line distorts the profile of F and obscures the useful satellites q and r. Therefore we do not feel that this spectrum can give us a meaningful measurement of R. G, being the ratio of two approximately equal numbers, is not severely affected by small errors in either. Thus we are able to provide an estimate of G. By basing the satellite line corrections on the Mg XI observations and the data for Mg XI and Si XIII in Bhalla, Gabriel, and Presnyakov (1975), we found G = 0.75 ± 0.07. This is lower than Pradhan's (1982) plotted value of 0.85 for $G(T_m)$.

For Si XIII we have only one suitable spectrum, the 1981 May 5, 14:10 UT SOLEX A spectrum. The SOLEX B detector is a glass channel-electron-multiplier array with a sharp change in efficiency at the silicon K absorption edge which, at 6.738 Å, almost overlies the F line wavelength of 6.739 Å. As a result, the F line flux is underestimated and neither R nor G can be determined. This peculiarity might be put to good use to measure Doppler shifts. We estimate that bulk velocities of 80 km s^{-1} should be easily detectable, but we have not yet observed them. We have only a small amount of data in the appropriate operational mode for this observation.

The Si XIII spectrum is shown in Figure 3c. The correction for satellite line emission was made as with Mg XI. In addition, the Mg XII 1s ^2S - 4p ^2P line, with wavelength 6.740 Å (Garcia and Mack, 1965) is blended with F. On the basis of the measured strength of the Mg XII 1s ^2S - 3p ^2P line we estimate that 15% of the apparent F flux is due to Mg XII. After making this correction we found R = 2.59 ± 0.60 and G = 0.60 ± 0.07. The R value is consistent with Pradhan's (1982) result of $R_0(T_m) \approx 2.6$, but the standard error is large. G is significantly below Pradhan's $G(T_m) \approx 0.85$. If the Mg XII correction were not made we would have found R = 2.98 and G = 0.67, so this correction does not account for the discrepancy between the theoretical and observational G values. Since this spectrum was taken at flare onset, the low G value may indicate that the temperature was high or that the plasma was in an ionizing state. The Mg XI spectrum taken near this time also gave a low G ratio.

V. SUMMARY

We have presented a compilation of spectral lines in the wavelength range 5.5 - 12 Å from observations under a variety of solar conditions, including flare onset (high temperature), flares, and nonflaring active regions. The wide range of solar conditions observed was of considerable value in line identification.

The lines of Fe XXII - XXIV are of particular interest in the analysis of flare plasmas because they are present at high temperatures. The line fluxes and wavelengths for these species were compared with theory. The comparison in Fe XXII was complicated by disagreement among past calculations of the wavelengths. For Fe XXIII and XXIV the wavelengths agreed with theoretical determinations. A general statement cannot be made about the relative strengths of lines emitted by a single species. Even when only the strongest lines were considered, some relative strengths agreed with theory and some did not. For these two species, n = 4-2 transitions are potentially useful in flare plasma analysis, but theoretical line strength calculations are lacking.

Finally, we treated the diagnostically useful line ratios of Mg XI, Al XII, and Si XIII. The density-sensitive line ratio, R, measured for Mg XI and Si XIII, agreed with theoretical

PREVIOUS PAGE IS BLANK

calculations of R_0, the low-density limit of R. For Mg XI in a flare-onset spectrum, R was lower than R_0 but the statistical significance of this result was not high. We suggested that Mg XI R measurements might be distorted by the presence of an Fe XXII line blended with the Mg XI intercombination line. The line ratio G was determined for all three helium-like species mentioned above. In each case the measured value was lower than the theoretical one. Similar results were found by us for Ne IX (McKenzie and Landecker 1982b) and by the Solar Maximum Mission observers for Ne IX, Mg XI, and (marginally) S XV (Wolfson et al. 1983). G ratios for Mg XI and Si XIII near flare onset were especially low. This could be because the temperature was high or the plasma was in an ionizing state, or both.

This work was supported by the U. S. Air Force Space Division under contract F04701-83-C-0084 and by the Aerospace-Sponsored Research program.

REFERENCES

Acton, L. W. and Brown, W. A. 1978, Ap. J., 225, 1065.

Bhalla, C. P., Gabriel, A. H., and Presnyakov, L. P. 1975, M.N.R.A.S., 172, 359.

Bhatia, A. K. and Mason, H. E. 1981, Astr. Ap., 103, 324.

Boiko, V. A., Faenov, A. Ya., and Pikuz, S. A. 1978, J. Quant. Spectrosc. Rad. Trans., 19, 11.

Bromage, G. E., Cowan, R. D. Fawcett, B. C., Gordon, H., Hobby, M. G., Peacock, N. J., and Ridgeley, A. 1977a, Culham Laboratory CLM-R170 (H. M. Stationery Off).

Bromage, G. E., Cowan, R. D. Fawcett, B. C., and Ridgeley, A. 1978, J. Opt. Soc. Am., 68, 48.

Bromage, G. E., Fawcett, B. C., and Cowan, R. D. 1977b, M.N.R.A.S., 178, 599.

Bromboszcz, G., Siarkowski, M., Sylwester, J., Korneev, V. V., Mandelshtam, S. L., Oparin, S. N., Urnov, A. M., and Zhitnik, I. A. 1983, Solar Phys., 83, 243.

Cohen, L. and Feldman, U. 1970, Ap. J. (Letters), 160, L105.

Doschek, G. A., Feldman, U., Landecker, P. B., and McKenzie, D. L. 1981, Ap. J., 249, 372.

Doschek, G. A., Meekins, J. F., and Cowan, R. D. 1972, Ap. J., 177, 261.

Doyle, J. B., Tayal, S. S., and Kingston, A. E. 1983, M.N.R.A.S., 203, 31P.

Ermolaev, A. M. and Jones, M. 1973, British National Reference Library, Ref. No. SUP 70009.

Fawcett, B. C. and Hayes, R. W. 1975, M.N.R.A.S., 170, 185.

Fawcett, B. C., Ridgeley, A., and Hughes, T. P. 1979, M.N.R.A.S., 188, 365.

Gabriel, A. H. 1972, M.N.R.A.S., 160, 99.

Gabriel, A. H. and Jordan, C. 1969, M.N.R.A.S., 145, 241.

Garcia, J. D. and Mack, J. E. 1965, J. Opt. Soc. Am., 55, 654.

Gordon, H. Hobby, M. G., and Peacock, N. J. 1980, J. Phys. B., 13, 1985.

Hayes, M. A. 1979, M.N.R.A.S., 189, 55P.

Hutcheon, R. J., Pye, J. P., and Evans, K. D. 1976, Ast. Ap., 51, 451.

Jacobs, V. L., Davis, J., Kepple, P. C., and Blaha, M. 1977, Ap. J., 211, 605.

Jacobs, V. L., Davis, J., Rogerson, J. E., Blaha, M., Cain, J., and Davis, M. 1980, Ap. J., 239, 1119.

Keenan, F. P., Tayal, S. S., and Kingston A. E. 1984, Solar Phys., 92, 75.

Krutov, V. V., Korneev, V. V., Karev, U. I., Lomkova, V. M., Oparin, S. N., Urnov, A. M.,, Zhitnik, I. A., Bromboszcz, G., Siarkowski, M., Sylwester, J., and Vasha, S. 1981, Solar Phys., 73, 105.

Landecker, P. B., McKenzie, D. L., and Rugge, H. R. 1979, Proc. Soc. Photo-Opt. Instrum. Eng., **184**, 285.

Mason, H. E., and Bhatia, A. K. 1983, Ast. Ap. Supp. Ser., **52**, 181.

Mason, H. E. and Storey, P. J. 1980, M.N.R.A.S., **191**, 631.

McKenzie, D. L., Broussard, R. M., Landecker, P. B., Rugge, H. R., Young, R. M. Doschek, G. A., and Feldman, U. 1980a, Ap. J. (Letters), **238**, L43.

McKenzie, D. L. and Landecker, P. B. 1981, Ap. J., **248**, 1117.

McKenzie, D. L. and Landecker, P. B. 1982a, Ap. J., **254**, 309.

McKenzie, D. L. and Landecker, P. B. 1982b, Ap. J., **259**, 327.

McKenzie, D. L., Landecker, P. B., Broussard, R. M. Rugge, H. R., Young, R. M., Feldman, U., and Doschek, G. A. 1980b, Ap. J., **241**, 409.

Mori, K., Otsuka, M., and Kato, T. 1979, Atomic Data and Nuclear Data Tables, **23**, 195.

Neupert, W. M., Swartz, M., and Kastner, S. O. 1973, Solar Phys., **31**, 171.

Parkinson, J. H. 1975, Solar Gamma-, X-, and EUV Radiation (Dordrecht, Holland: D. Reidel), 45.

Phillips, K. J. H., Leibacher, J. W., Wolfson, C. J., Parkinson, J. H., Fawcett, B. C., Kent, B. J., Mason, H. E., Acton, L. W., Culhane, J. L., and Gabriel, A. H. 1982, Ap. J., **256**, 774.

Pradhan, A. K. 1982, Ap. J., **263**, 477.

Pradhan, A. K., Norcross, D. W., and Hummer, D. G. 1981, Phys. Rev. A, **23**, 619.

Pradhan, A. K., and Shull, J. M. 1981, Ap. J., **249**, 821.

Reader, J., and Sugar, J. 1975, J. Phys. Chem. Ref. Data, **4**, 353.

Siarkowski, M., Sylwester, J., Bromboszcz, G., Korneev, V. V., Mandelshtam, S. L., Oparin, S. N., Urnov, A. M., Zhitnik, I. A., and Vasha, S. 1982, Solar Phys., **77**, 183.

Summers, H. P. 1973, Ap. J (Letters), **179**, L45.

Swartz, M., Kastner, S., Rothe, E., and Neupert, W. 1971, J. Phys. B, **4**, 1747.

Wolfson, C. J., Doyle, J. G., Leibacher, J. W., and Phillips, K. J. H. 1983, Ap. J., **269**, 319.

LABORATORY OPERATIONS

The Laboratory Operations of The Aerospace Corporation is conducting experimental and theoretical investigations necessary for the evaluation and application of scientific advances to new military space systems. Versatility and flexibility have been developed to a high degree by the laboratory personnel in dealing with the many problems encountered in the nation's rapidly developing space systems. Expertise in the latest scientific developments is vital to the accomplishment of tasks related to these problems. The laboratories that contribute to this research are:

Aerophysics Laboratory: Launch vehicle and reentry fluid mechanics, heat transfer and flight dynamics; chemical and electric propulsion, propellant chemistry, environmental hazards, trace detection; spacecraft structural mechanics, contamination, thermal and structural control; high temperature thermomechanics, gas kinetics and radiation; cw and pulsed laser development including chemical kinetics, spectroscopy, optical resonators, beam control, atmospheric propagation, laser effects and countermeasures.

Chemistry and Physics Laboratory: Atmospheric chemical reactions, atmospheric optics, light scattering, state-specific chemical reactions and radiation transport in rocket plumes, applied laser spectroscopy, laser chemistry, laser optoelectronics, solar cell physics, battery electrochemistry, space vacuum and radiation effects on materials, lubrication and surface phenomena, thermionic emission, photosensitive materials and detectors, atomic frequency standards, and environmental chemistry.

Electronics Research Laboratory: Microelectronics, GaAs low noise and power devices, semiconductor lasers, electromagnetic and optical propagation phenomena, quantum electronics, laser communications, lidar, and electro-optics; communication sciences, applied electronics, semiconductor crystal and device physics, radiometric imaging; millimeter wave, microwave technology, and RF systems research.

Information Sciences Research Office: Program verification, program translation, performance-sensitive system design, distributed architectures for spaceborne computers, fault-tolerant computer systems, artificial intelligence and microelectronics applications.

Materials Sciences Laboratory: Development of new materials: metal matrix composites, polymers, and new forms of carbon; nondestructive evaluation, component failure analysis and reliability; fracture mechanics and stress corrosion; analysis and evaluation of materials at cryogenic and elevated temperatures as well as in space and enemy-induced environments.

Space Sciences Laboratory: Magnetospheric, auroral and cosmic ray physics, wave-particle interactions, magnetospheric plasma waves; atmospheric and ionospheric physics, density and composition of the upper atmosphere, remote sensing using atmospheric radiation; solar physics, infrared astronomy, infrared signature analysis; effects of solar activity, magnetic storms and nuclear explosions on the earth's atmosphere, ionosphere and magnetosphere; effects of electromagnetic and particulate radiations on space systems; space instrumentation.

DATE
ILMED
-8